

Decomposing the Deep: Finding Class Specific Filters in Deep CNNs

Akshay Badola¹, Cherian Roy², Vineet Padmanabhan³, and Rajendra Lal⁴

^{1,2,3,4} School of Computer and Information Sciences, Univeristy of Hyderabad, Prof C R Rao Road, Gachibowli, Hyderabad, 500019, Telangana, India

¹badola@uohyd.ac.in

²cherianthakidiyel@gmail.com

³vineetnair@uohyd.ac.in

⁴rpls@uohyd.ernet.in

January 5, 2022

Abstract

Interpretability of Deep Neural Networks has become a major area of exploration. Although these networks have achieved state of the art accuracy in many tasks, it is extremely difficult to interpret and explain their decisions. In this work we analyze the final and penultimate layers of Deep Convolutional Networks and provide an efficient method for identifying subsets of features that contribute most towards the network's decision for a class. We demonstrate that the number of such features per class is much lower in comparison to the dimension of the final layer and therefore the decision surface of Deep CNNs lies on a low dimensional manifold and is proportional to the network depth. Our methods allow to decompose the final layer into separate subspaces which is far more interpretable and has a lower computational cost as compared to the final layer of the full network.

Keywords: Deep Learning, Convolutional Neural Networks, Interpretable CNNs, Disentanglement

1 Introduction

Deep Neural Networks have been a paradigm shift in machine learning but they have remained primarily black boxes. Large networks can contain millions [21],

[8] to billions [19], [2] of parameters. Such models are highly overparameterized and in fact, overparameterization is essential to their generalization ability [3], [5], [4]. In such cases it becomes extremely difficult to attribute the prediction of any network to its parameters which leads to poor understanding and interpretability of the network. The lack of interpretability of these models makes it very difficult for humans to trust those models in critical situations, like medical diagnosis or self-driving vehicles. It also becomes very hard to diagnose and correct the models themselves.

Final layers¹ of a CNN hold particular interest for interpretability as detectors that appear there are more aligned with semantic concepts. The final layer of the network projects the features via softmax onto the decision simplex and its properties are critical to the final label predicted by the network.

While there has been recent work in interpreting and disentangling neural network features; in the current literature we have not come across an efficient method to identify and rank the features in the final and penultimate layers and consequently decompose the layer. In this work we focus on the final and penultimate layers of some popular CNN architectures, namely Resnet [8], Densenet [9], Efficientnets [23]. We illustrate some properties of those layers and consequent features and provide an efficient method to decompose the final layer which results in interpretability via disentanglement and reduces the computational complexity of the final layer. We also provide the implementation for decomposing the final layers².

2 Related Work

For any model, interpretation should result in some attribution from the parameters of the model towards the predictions made by it. This is separate than *distilling* a network into a more explainable model like a decision tree [6], which aims more towards converting the model to a simpler one. Model interpretation (and consequent simplification) on the other hand, does not attempt to significantly alter the model.

2.1 CNN Interpretability

There is sufficient prior work on inspecting and transferring the filters in a Deep CNN. A detailed survey is given in [28]. Earlier works like [27], [22], [20], analyzed the filters in intermediate layers and found that the features from pretrained neural networks can be used for other tasks.

¹When we say final layer(s) we mean the layers closer to the classifying layer. Following previous works we also mention them as *top* layer(s) and the layers closer to input as *bottom* layer(s).

²<https://github.com/akshaybadola/cnn-class-specific-filters-with-histogram>

Later work has moved more towards class attribution and aligning features to semantic concepts. Gonazalz-Garcia et. al. [7] and Bau et. al. [1] analyze the activation maps of CNNs and discover that the final layers of the networks align closer to semantic concepts than the early layers which were more attuned to detecting texture and color.

We focus on the line of investigation looking for feature importance in CNNs and sparse CNNs. Liu et. al. [18] use sparse low rank decompositions in pretrained CNNs. Li et. al. [14] use ℓ_1 norm of filters to rank the convolutional filters as a whole and prune the less important ones. Kumar et. al. [13] also use ℓ_1 norm with a *capped* ℓ_1 norm to formulate classification with CNNs as a *lasso* like problem. Lin et. al. [17] introduce a *structured sparsity regularization*. Li et. al. [15] introduce a *kernel sparsity and entropy* (KSE) measure which quantifies both sparsity and diversity of the convolution kernels. Liang et. al. [16] use sparsity to find out the important filters in a CNN, though instead of going towards a parameter level sparsity like dropout or quantization [25], they look at one Convolutional Filter as a single parameter.

The notion of *class specificity* is explored in Wang et. al. [24]. They try to increase accuracy with filters that capture *class-specific* discriminative patches. These *class-specific* filters are closely related to earlier work in Jiang et. al. [11], who introduce the concept of *Label Consistent Neural Networks* to learn features which they claim alleviate gradient vanishing and leads to faster convergence. [16] try to use sparsity to find out the important filters which they claim are also *class specific*.

2.2 Our Contributions

Our work takes inspiration from [14], [24] and [16]. We combine the ideas of *class specificity* [24], [16] and ℓ_1 norm based filter importance [14] to arrive at a method for identifying the k most influential features based on an ℓ_1 norm importance metric in the final and penultimate layers of a CNN and demonstrate its efficacy with experiments on various CNNs.

In particular:

1. We show that only a few filters *per class* are needed to make a decision for a deep CNN.
2. We provide an algorithm to obtain those filters from *any pre-trained* network with a single fully connected layer.
3. We demonstrate the relation between depth and filter disentanglement in CNNs and show that deeper networks lead to lower dimensional representations in the final layer.

The rest of the paper is organized as follows: We discuss CNNs and the concept *class specific features* in Section 3. We provide an overview of analysis of

techniques on final layer and *class specific features* therein, in Section 4. We describe the experimental details and results in Section 5. We discuss implications and future scope in Section 6.

3 Background

We discuss CNNs, filters and layers in the next sections and establish notation which will aid us in our describing our methods.

3.1 Notation

Let $\{(\mathcal{X}, \mathcal{Y})\}$ be the set of data tuples. An instance of the data $(X, y) \in \{(\mathcal{X}, \mathcal{Y})\}$ is a tuple of (image, label) with $X \in \mathbb{R}^{c \times h \times w}$ where c, h, w are the channels, height and width of the image respectively. y is an integer response variable representing one of the n classes, $y \in \mathbb{Z}^+, 0 \leq y < n$. y can also be represented as an index vector indexing the i^{th} class, $y \in \{0, 1\}^n : y = i \equiv \{0, 0, \dots, 1, \dots, 0\}$.

Formally a Deep Neural Network is a set of weights which act as a sequence of operators on input X , such that, $y = \mathcal{A}W^d(\dots\mathcal{A}W^1(\mathcal{A}W^0(X)))$ where W^d is a weight tensor at depth d and \mathcal{A} is an element-wise function also known as an *activation function*. While the activation function \mathcal{A} need not be same for each weight W^d for CNNs that we consider, only RELU $\max(0, x)$ is used. An exception is the weights at the end of the network where a softmax $\sigma(x) = \exp(x_j) / \sum \exp(x_j)$ is used.

A *layer* of a network is a single weight+activation operation $O^d = \mathcal{A}(W^d(I^d))$ where I^d, W^d, O^d are input, weights and output at depth d . We will denote the layer at depth d as L^d .

3.1.1 CNNs

A Convolutional Network consists of filter banks of *convolution* (or cross correlation) filters which are square matrices of odd rank acting on the input with an element-wise activation function on the output. Such an output O^d at layer d is called a *feature map* at d^{th} layer. Filters are the fundamental unit for a CNN and it is convenient to represent and analyze a CNN as operations due to the filters. For our purposes, we will denote the j^{th} filter for layer i as L_j^i .

Modern Deep CNNs rely heavily on RELU and Batch Normalization [10] in the intermediate layers. Batch Normalization and RELU are performed after the Convolution operator and the entire unit can be considered as a single operator. We refer the reader to [12], [21] and [8] for internals of CNNs.

3.2 Filter Disentanglement and Label Consistency

As mentioned earlier, the sheer number of features and the layers in CNNs makes them very hard to interpret. One approach towards their interpretation is *Filter*

Disentanglement. Filter Disentanglement refers to the fact that the filters in a CNN should represent separate concepts. As concepts in a network are hard to identify, we can instead use the attribution of a filter towards the prediction of a label as a surrogate measure of disentanglement. *Ideally* every filter should be responsible for detection of a particular pattern in the image, but that is difficult in practice. In particular at the bottom layers the filters are highly entangled and learn very generic features [1]. As we move up the network, at the top layers they tend to be less entangled but not entirely so.

As in Section 3.1.1, the set of filters for a CNN at depth d constitutes the layer L^d . Now consider a single label $y \in \mathcal{Y}$. Let $\exists L_{J_y}^d \subset L^d$ where J_y is an index set such that, $L_{J_y}^d$ alone is responsible for the prediction of label y .

For such a set J_y , we define the *influence* relation \prec for the probability $P(y^d)$ of a label y at depth d of a CNN as: $P(y^d) \prec L_{J_y}^d$. We say that the features $L_{J_y}^d$ are *influential* at depth d for the prediction of label y .

We will focus only on the final layer so we can remove the superscript d without ambiguity. To enforce disentanglement and considering only the final layer we should ideally have,

1. $|L_{J_y}| \ll |L|, \forall y$ and,
2. $L_{J_{y_1}} \neq L_{J_{y_2}}, \forall y_1, y_2 \in \mathcal{Y}$

That is, the filters at depth d for each class y should be disjoint. However, as we mentioned above, that is not practically feasible. Instead we can hope to find:

1. $|L_{J_y}| \ll |L|, \forall y$
2. $\operatorname{argmin}_{J_{y_1}, J_{y_2}} (L_{J_{y_1}} \cap L_{J_{y_2}}), \forall y_1, y_2 \in \mathcal{Y}$

Or we should seek index sets J_{y_i} such that there is minimal overlap between two classes. These *class-specific* filters are closely related to [11], except that [11] associate a *neuron* (or weight) with a label while we associate filters. The *class-specific* filters discussed in Liang et. al. [16] are more similar to these. However, unlike [16] and [24] our method does not require supervision and can be used for any pretrained network. And, although we use ℓ_1 norm to identify filters, our method identifies *class specific* filters and decomposes the final layer while the method in [14] does not.

4 Influential Features

The penultimate and final layers are of particular interest in feature attribution in CNNs as they contain the final representation of the image and directly lead to the prediction of the label, while the lower layers learn the filters which respond to textures and lower level features [1]. Here we describe the various factors in determining the *influential features* in the final layer.

4.1 ℓ_1 norm for Feature Importance

Previously [14] and [16] have both used ℓ_1 norm for estimating filter importance. However, earlier works such as the two above, do not explicitly discover a lower dimensional decision surface. Following [14] and [16] we look at the ℓ_1 norm of the resulting *features per class* as the primary differentiating factor.

One approach would be to check the ℓ_1 norm of *weights* in the final and pre final layers which is similar to [16]. However we can note that the ℓ_1 norm of the weights will not vary for each class so it is much harder to identify *class specific* features with that. In our initial experiments also, this hypothesis was verified.

Another key observation we make is that all the features in the entire CNN are ≥ 0 because of RELU. In effect the feature vectors/tensors are positive semidefinite, which means that the ℓ_1 norm of each feature directly contributes to the classification output of the final layer. The weights on the other hand are roughly 50% ≥ 0 and 50% ≤ 0 and therefore it's easier to quantify feature importance than weight importance with ℓ_1 norm.

4.2 Separating Outputs for each Class

A second insight we had is that the final layer output *for each class* is the result of a dot product between features for that class and weights for that class. Therefore the final layer can be thought of as c separate dot products, where $c = |\mathcal{Y}|$ as earlier is the number of classes. Hence, selecting certain features *for each class* will not affect the output for the other.

Formally, $P(y|X) = O^d = \sigma(WI^d)$ as in Section 3.1.1, where $O^d \in \mathbb{R}^n$ and $\sum_i O_i^d = 1$. If we omit d and X for simplicity, then probability for i^{th} class, $P(y = i)$ is the value of i^{th} component of the output from the final layer, which is O_i .

Now the final layer is a single matrix, so O_i is simply the dot product of i^{th} row of the weight matrix W with the input feature vector I . If m is the *width* of the final layer then, $O_i = W_i \cdot I$, where $W \in \mathbb{R}^{m \times n}$ and $W_i, I \in \mathbb{R}^m$.

Now, let $\mathbf{w}_{k,i}$ be the k dimensional subspace of W_i for the index i , that is, $\mathbf{w}_{k,i} \subset W_i$, $\mathbf{w}_{k,i} \in \mathbb{R}^k$, $k \ll m$. Then we define the probability for label i at final layer with reduced dimension k as $P(y^k = i) = \sum \mathbf{w}_{k,i} I_k$.

Recall that the predicted label with the full *width* is $\hat{y} = \text{argmax}(y)$. We define a prediction with reduced dimension k as $\hat{y}_k = \text{argmax}(y_k)$. The goal then is to find such $\mathbf{w}_{k,i}$ for each class i , such that the difference in the predictions $d(\hat{y}_k, \hat{y})$ is minimized, where d is some metric.

That is, \mathbf{w}_k are the truncated weights which minimize the difference between the predicted labels at *width* k and predicted labels at full *width* n for each class.

4.3 Finding the Influential Features

We note that finding the *class specific influential features* $\mathbf{w}_{k,i}$ is non-trivial as the exact subset of the weights cannot be known easily. However, as we mention in Section 4.1 ℓ_1 norm of the features can help us in guiding towards the correct set of filters.

In our experiments we found that although selecting weights by top ℓ_1 norm would result in *weights attribution*, it would not result in *class specific features attribution*. Instead searching for *topk features per class* with ℓ_1 norm gave us better results. Even combining *topk filters per class* with *topk weights* led to poorer results than with *topk features per class*.

A problem though is that, the features per instance vary across a single class, and the label of the instance cannot be known in advance. However a *topk selection from histogram of topk features for all instances* in a given class had mass concentrated around a few points, which corresponded to such *influential features*. We give the details of the algorithm in the next section.

4.4 Algorithm

Here we discuss the algorithm to obtain the k most *influential features* for each class from a pretrained CNN. For the algorithm 1 below, \mathcal{I} are the set of features at final layer for all classes, where we omit the layer superscript used earlier for simplicity. Denote the set of features for label y by I_y . We want to obtain the mapping $\mathbb{I} : y \rightarrow I_y$, such that, $\mathbb{I}(y)$ gives the most influential features for class y . The parameters for the algorithm are $k_1, k_2 \in \mathbb{Z}^+$ which define the initial and subsequent feature selection, which we describe below.

We proceed by noting top k_1 features by ℓ_1 norm of each data instance for *each class* at the pre-final layer and select the indices in a set $I_y^{topk_1}$ for class y . We set $k_1 \ll m$ where m is the dimension of the features at the pre-final layer (and hence, also the dimension of the final layer). E.g., if for a 64 dimensional feature vector, let the top 5 components sorted by ℓ_1 norm occur at indices $< 3, 5, 14, 18, 28 >$. Then the index set for $k_1 = 5$ for the entire class is aggregation $\uplus I_y^{top5}$ of all such sets, where \uplus is an aggregation operator, e.g. $\uplus < 3, 5 > < 3, 14 > = < 3, 3, 5, 14 >$

The set $\uplus I_y^{topk}$ then denotes all the occurrences of a particular dimension (or index) of a feature in *topk* ℓ_1 norm set, for a class in pre-final layer. From the frequency histogram of each class we then select the top k_2 most frequent indices.

We also experimented with k_1 which covers a certain percentage (say 90%) of contribution of the filters. However, we found that a value of 5 for CIFAR-10 and 50 for Imagenet datasets gave us 90% coverage, which we then chose to set for all our experiments as that is faster to implement.

HIST in algorithm 1 refers to the histogram of frequencies of each index.

Algorithm 1 Extract Influential Features

```
1: Input:  $\mathcal{I}, \mathbb{I}, k_1, k_2$ 
2: Output: Mapping  $\mathbb{I}$  of Influential Features
3: procedure GET_INDICES( $\mathcal{I}, y$ )
4:   for  $I_y \leftarrow \mathcal{I}$  do
5:     for  $i_y \leftarrow I_y$  do
6:        $I_y^{topk_1} = I_y^{topk_1} \uplus (\text{sorted}_k(i_y))$  w.r.t.  $\ell_1$  norm
7:     end for
8:      $\mathbb{I}_y \leftarrow \text{topk}_2(\text{HIST}(I_y^{topk_1}))$ 
9:      $\mathbb{I} = \mathbb{I} \uplus (y, \mathbb{I}_y)$   $\triangleright (y, \mathbb{I}_y)$  is a tuple of  $y$  and  $\mathbb{I}_y$ 
10:   end for
11: end procedure
```

5 Experiments and Results

We conducted some initial experiments on Class Specific Gates (CSG) [16] and we discuss them in 5.1 as to illustrate our argument. We then analyze and discuss the efficacy of our proposed *influential features* in 5.2. As mentioned earlier, we take inspiration from [14] and [16] and combine class specificity with ℓ_1 norm importance. We note that while [16] is a supervised method, their approach is closest to ours in principle. [14] is unsupervised but their aim is to induce sparsity and not interpretability. Also their approach doesn't lead to explicit class specific disentanglement. We demonstrate that **our unsupervised approach** gives a) good if not better results than [16] b) leads to explicit filter disentanglement c) reduces computational cost in the final layer.

5.1 Class Specific Filters

We first discuss experiments with *class specific gates* (CSG). Liang et. al. [16] had proposed to learn a matrix $\text{CSG} \in \mathbb{R}^{m \times n}$ where m is the dimension of final layer and $c = |\mathcal{Y}|$ is the number of classes. See [16] for details of the training procedure. One important issue to consider with [16] is that the label CSG matrix would not be available when doing inference as the labels for new data is not known. Hence it can only be used to interpret a CNN on a given dataset and cannot be used for any new data. We implement CSG and summarize the results in Table 1.

STD output in the Table 1 is $O_i^{STD} = O_i^d = \sigma(WI^d)_i$, which is the same as CNN output without a CSG matrix. Output using CSG matrix is $O_i^{CSG} = \sigma(W(I^d \odot \text{CSG}_i))$, where \odot denotes the Hadamard or element-wise product. We note that the CSG accuracy is similar to the STD accuracy. CSG and STD are CSG and STD output paths respectively.

Table 1: CSG Experiments Conducted by us

Dataset	Model	Training	Accuracy
CIFAR-10	Resnet20	CSG	0.8809
		STD	0.8809
	Resnet34	CSG	0.8407
		STD	0.8407
Tiny Imagenet 200	Resnet18	CSG	0.3633
		STD	0.3641
	Resnet34	CSG	0.3794
		STD	0.3852

5.2 Influential Features

We then performed experiments to obtain *influential filters* according to Algorithm 1 for datasets CIFAR-10 and Imagenet, and families of models a) Resnet b) Densenet c) Efficientnet to demonstrate that our method can work for any CNN.

Resnet [8] are the most popular variants of CNNs because of their lower computational cost and good generalization in spite of it. Densenets [9] are another popular architecture which connect each layer to every other layer. Efficientnets [23] are recent models which are developed with Neural Architecture Search [29] and aim to reduce the computational cost while preserving accuracy.

CIFAR-10 consists of 50,000 training images for 10 classes, i.e., $c = |\mathcal{Y}| = 10$, of size 32×32 and 10,000 validation images. Imagenet has 1,000,000 images of varying sizes with $c = 1000$ but while training they are resized to 224×224 . The validation split has 50,000 images for Imagenet. For both the datasets and all the models we determine k_1, k_2 and $\biguplus I^{topk}$ only from the training set. The results are then calculated on the validation set.

5.2.1 Effect of k_1 and k_2

We conduct a detailed study on Resnet20 model and CIFAR-10 dataset to analyze the effect of values of k_1 and k_2 on the resulting model. For the Resnet20 model, our pretrained model had accuracy 91.17. We measure the efficacy of the resulting decomposed final layer as the ratio $r_A = \frac{A_d}{A_f}$, where A_d, A_f are the decomposed and full width accuracies respectively. See Fig 1 for the results.

We observe overall that reducing the dimensionality by lowering the number of input features to the final layer also results in a reduction of accuracy. This is to be expected as we are losing information at the last layer. We note that even for $k_2 = 3$, we get 84.16 accuracy which is pretty good for only 3 filters per class. This confirms that the decision surface lies on a much lower dimensional subspace than the dimension of the final layer.

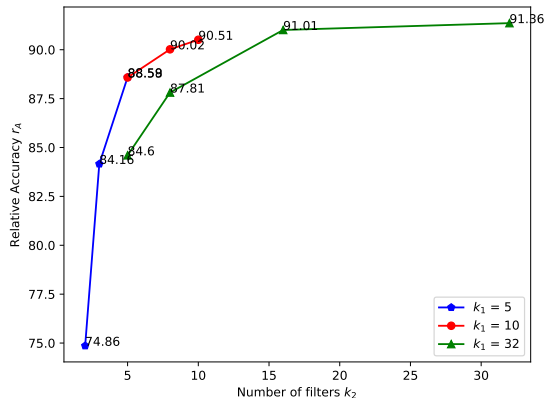


Figure 1: Effect of k_1 and k_2 on Accuracies for Resnet20 and CIFAR-10

Table 2: Effect of depth on Resnet variants

	Resnet50	Resnet101	Resnet152
Final Dim n	2048		
k_2/c	0.05		
k_2/n	0.0244141		
A_d	0.64792	0.68164	0.69346
A_f	0.74548	0.75986	0.77014
r_A	0.869131	0.89706	0.900434

Another thing we can note is that, for a given value of k_1 the best results are obtained by setting $k_2 = k_1$. Also, if initial filter selection k_1 is very large, then equivalent k_2 setting leads to lower performance as compared to a lower k_1 .

5.2.2 Effect of Depth

Here we discuss the results of experiments on various other models including variants of Resnet. For all the following experiments we use Imagenet Dataset and set $k_1 = k_2 = 50$. Two important metrics in experiments with depth are k_2/n and number of filters per class k_2/c . For all variants of Resnet $k_2/n, k_2/c$ and dimension of final layer n remain the same. Table 2 summarizes the results for Resnet models.

We can see that the relative accuracy r_A drops for Imagenet in these variants compared to Resnet20, but the number of filters per class k_2/c is also lower at 0.05 as compared to 0.5 for Resnet20 which is an order of magnitude. k_2/n is also lower at 0.024 as compared to 0.078. This is due to the much higher number of classes in the Imagenet dataset. Apart from that the effect of r_A on depth is clear as it increases monotonically with increasing depth.

Table 3: Effect of depth on Wide Resnet

	Wide Resnet 50	Wide Resnet 101
Final Dim n	2048	
k_2/c	0.05	
k_2/n	0.0244141	
A_d	0.75008	0.75988
A_f	0.77256	0.77908
r_A	0.970902	0.975356

Table 4: Effect of depth on Densenet 121 and 169

	Densenet121	Densenet169
Final Dim n	2048	
k_2/c	0.05	
k_2/n	0.0488281	0.0300481
A_d	0.6372	0.66328
A_f	0.71956	0.73754
r_A	0.885541	0.899314

We also evaluate on Wide Resnets [26] which contain a greater number of convolution filters per layer as compared to standard Resnet models. We get a much higher relative accuracy r_A on these as compared to standard Resnets for the same number of layers (see Table 3). We suspect that the greater number of convolutional filters help in disentanglement as there are more filters per class in the previous layers.

For all the models we can see that across a class of models r_A increases with depth. Only EfficientNet deviates from this behaviour which we discuss later. Densenets [9] have different n and hence k_2/n differs for them. For Densenets we compare Densenet121 with Densenet169 and Densenet161 with Densenet201, as the two pairs have closer n and hence k_2/n .

Coming to Densnets, we can see a similar trend of increasing r_A with depth (Tables 4, 5). The r_A here is comparable to that of Resnets but not Wide Resnet

Table 5: Effect of depth on Densenet 121 and 169

	Densenet161	Densenet201
Final Dim n	2048	
k_2/c	0.05	
k_2/n	0.0226449	0.0260417
A_d	0.6766	0.68214
A_f	0.75268	0.7455
r_A	0.898921	0.91501

Table 6: Effect of depth on Efficientnet variants

	efficientnet_b0	efficientnet_b1	efficientnet_b2	efficientnet_b3
Final Dim n	1280	1280	1408	1536
Num Layers	82	116	116	131
k_2/c	0.05	0.05	0.05	0.05
k_2/n	0.0390625	0.0390625	0.0355114	0.0325521
A_d	0.64838	0.7046	0.6778	0.64842
A_f	0.7609	0.76392	0.76762	0.76928
r_A	0.852122	0.922348	0.882989	0.842892

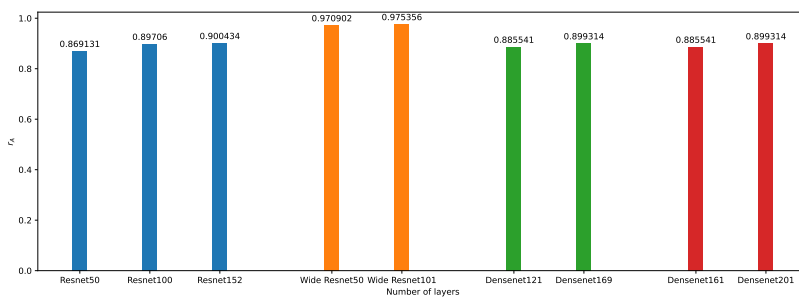


Figure 2: Effect of number of layers (depth) of a network with Relative Accuracy r_A . We can see that r_A increases with depth for a class of models.

variants. The final layer dimension n also differs for Densenets so we compare models with a similar n . We can see that r_A tends to increase with depth which shows the effect of depth on filter disentanglement. See Figure 2 for a summary of r_A on all models.

Only with Efficientnets (Table 6), which are NAS based models, do we see a deviation from this pattern as their model architecture differs from human designed networks. With Efficientnets, as the number of layers increases from 82 to 116 we see a corresponding jump in r_A except *efficientnet_b2* which has same number of layers as *efficientnet_b1* but has a wider final layer, we see a drop in r_A . *efficientnet_b3* is a curiosity as that model is both deeper and wider.

5.2.3 Decomposition and Prediction with Influential Features

The computational cost of predicting with *influential features* is also less as only a few filters are needed for predicting a class. Because of identification of explicit *class specific filters* we can decompose the final layer into class specific subspaces. The network can then be retrained to recover the original accuracy. For Resnet20 and CIFAR-10 the accuracy drops to 88.59 with *influential features* with $k_1 = k_2 = 5$. After that, we can decompose the final layer so that each class has a separate subspace of features. After training for one epoch we get accuracy of 91.51, which is very close to the original accuracy of 91.71. An illustration of how efficient prediction with *influential features* works is given in Figure 3.

The computational complexity for the final layer is $d \times n$ where d is the dimension of the final layer and n is the number of classes. After using only *influential features* it drops significantly. For example for Resnet20 and CIFAR-10, the computational complexity for the final layer is 64×10 which drops to 5×10 with *influential features*.

6 Conclusion and Future Work

We have described here a novel method of identifying the k most influential features for the final layers of a CNN. The method allows us greater interpretability into the CNN and also to decompose the final layer into separate class specific final layer. We have also shown that deeper networks have inherently more disentangled representations in the final layers. Finally, we also provide the implementation for the experiments and the decomposed final layer computations.

For future work, the focus of the investigation can shift to inner layers of the CNN. We have also seen that the accuracy can also be recovered when trained for very few epochs for CIFAR-10. This raises the possibility of further hierarchical decomposition of the CNN as a tree like structure which can be explored in future work.

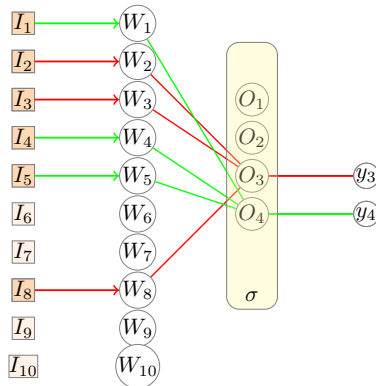


Figure 3: Prediction with influential features for class y_3, y_4 . For both only 3 input features are required and the probability for each is $\sigma(I_{inf} \odot W_{inf})$

Models like Efficientnet [23] give us different results as they are derived from Neural Architecture Search (NAS) which leads to more complex models and we can hypothesize that their representations are more entangled. Other models on the other hand are designed by human intuition and are simpler. However, that would require exploration of NAS based models which we also leave to future work.

7 Acknowledgements

We wish to thank the MEITY, Govt. of India, which funded part of this research with Visvesvaraya PhD Fellowship award number MEITY-PHD-1035.

References

- [1] D. Bau, B. Zhou, A. Khosla, A. Oliva, and A. Torralba. Network Dissection - Quantifying Interpretability of Deep Visual Representations. In *Proc. of the IEEE Conf. on Comput. Vis. and Pattern Recognit.*, pages 3319–3327, 2017.
- [2] T. B. Brown, B. Mann, N. Ryder, M. Subbiah, J. Kaplan, P. Dhariwal, A. Neelakantan, P. Shyam, G. Sastry, A. Askell, S. Agarwal, A. Herbert-Voss, G. Krueger, T. Henighan, R. Child, A. Ramesh, D. M. Ziegler, J. Wu, C. Winter, C. Hesse, M. Chen, E. Sigler, M. Litwin, S. Gray, B. Chess, J. Clark, C. Berner, S. McCandlish, A. Radford, I. Sutskever, and D. Amodei. Language Models Are Few - Shot Learners. In *Adv. in Neural Inf. Process. Syst.*, 2020.
- [3] A. Choromańska, M. Henaff, M. Mathieu, G. B. Arous, and Y. LeCun. The

- Loss Surfaces of Multilayer Networks. In *Proc. of the International Conf. on Artif. Intell. and Stat.*, volume 38, pages 192–204, nov 2015.
- [4] S. Du, J. Lee, H. Li, L. Wang, and X. Zhai. Gradient Descent Finds Global Minima of Deep Neural Networks. In *Proc. of the International Conf. on Mach. Learn.*, nov 2019.
- [5] S. Du, X. Zhai, B. Póczos, and A. Singh. Gradient Descent Provably Optimizes over - Parameterized Neural Networks. In *Proc. of the International Conf. on Learn. Represent.*, 2019.
- [6] N. Frosst and G. E. Hinton. Distilling a Neural Network into a Soft Decision Tree. In *Cex@ai*ia*, 2017.
- [7] A. Gonzalez-Garcia, D. Modolo, and V. Ferrari. Do Semantic Parts Emerge in Convolutional Neural Networks? *International J. of Comput. Vis.*, 126:476–494, jul 2017.
- [8] K. He, X. Zhang, S. Ren, and J. Sun. Deep Residual Learning for Image Recognition. In *Proc. of the IEEE Conf. on Comput. Vis. and Pattern Recognit.*, pages 770–778, 2016.
- [9] G. Huang, Z. Liu, and K. Q. Weinberger. Densely Connected Convolutional Networks. In *Proc. of the IEEE Conf. on Comput. Vis. and Pattern Recognit.*, pages 2261–2269, aug 2017.
- [10] S. Ioffe and C. Szegedy. Batch Normalization: Accelerating Deep Network Training by Reducing Internal Covariate Shift. In *Proc. of the International Conf. on Mach. Learn.*, feb 2015.
- [11] Z. Jiang, Y. Wang, L. Davis, W. Andrews, and V. Rozgic. Learning Discriminative Features via Label Consistent Neural Network. In *Proc. of the IEEE Winter Conf. on Appl. of Comput. Vis.*, pages 207–216, feb 2017.
- [12] A. Krizhevsky, I. Sutskever, and G. E. Hinton. Imagenet Classification with Deep Convolutional Neural Networks. In *Adv. in Neural Inf. Process. Syst.*, pages 1097–1105, 2012.
- [13] A. Kumar, A. M. Shaikh, Y. Li, H. Bilal, and B. Yin. Pruning Filters with L1 - Norm and Capped L1 - Norm for CNN Compression. *Applied Intell.*, 51:1152–1160, sep 2021.
- [14] H. Li, A. Kadav, I. Durdanovic, H. Samet, and H. Graf. Pruning Filters for Efficient ConvNets. In *Proc. of the International Conf. on Learn. Represent.*, 2017.
- [15] Y. Li, S. Lin, B. Zhang, J. Liu, D. Doermann, Y. Wu, F. Huang, and R. Ji. Exploiting Kernel Sparsity and Entropy for Interpretable CNN Compression. In *Proc. of the IEEE Conf. on Comput. Vis. and Pattern Recognit.*, 2019.

- [16] H. Liang, Z. Ouyang, Y. Zeng, H. Su, Z. He, S.-T. Xia, J. Zhu, and B. Zhang. Training Interpretable Convolutional Neural Networks by Differentiating Class - Specific Filters. In *Proc. of the Eur. Conf. on Comput. Vis.*, pages 622–638. Springer International Publishing, jul 2020.
- [17] S. Lin, R. Ji, Y. Li, C. Deng, and X. Li. Toward Compact ConvNets via Structure - Sparsity Regularized Filter Pruning. In *IEEE Trans. on Neural Networks and Learn. Syst.*, 2020.
- [18] B. Liu, M. Wang, H. Foroosh, M. Tappen, and M. Pensky. Sparse Convolutional Neural Networks. In *Proc. of the IEEE Conf. on Comput. Vis. and Pattern Recognit.*, pages 806–814, jun 2015.
- [19] A. Radford, J. Wu, R. Child, D. Luan, D. Amodei, and I. Sutskever. Language Models are Unsupervised Multitask Learners. https://cdn.openai.com/better-language-models/language_models_are_unsupervised_multitask_learners.pdf, 2019. Accessed: 2021-06-25.
- [20] K. Simonyan, A. Vedaldi, and A. Zisserman. Deep Inside Convolutional Networks: Visualising Image Classification Models and Saliency Maps. In *Proc. of the International Conf. on Learn. Represent.*, 2014.
- [21] C. Szegedy, W. Liu, Y. Jia, P. Sermanet, S. Reed, D. Anguelov, D. Erhan, V. Vanhoucke, and A. Rabinovich. Going Deeper with Convolutions. In *Proc. of the IEEE Conf. on Comput. Vis. and Pattern Recognit.*, pages 1–9, 2015.
- [22] C. Szegedy, W. Zaremba, I. Sutskever, J. Bruna, D. Erhan, I. Goodfellow, and R. Fergus. Intriguing Properties of Neural Networks. In *Proc. of the International Conf. on Learn. Represent.*, 2014.
- [23] M. Tan and Q. V. Le. Efficientnet: Rethinking Model Scaling for Convolutional Neural Networks. In *Proc. of the International Conf. on Mach. Learn.*, may 2019.
- [24] Y. Wang, V. I. Morariu, and L. Davis. Learning a Discriminative Filter Bank Within a CNN for Fine - Grained Recognition. In *Proc. of the IEEE Conf. on Comput. Vis. and Pattern Recognit.*, pages 4148–4157, nov 2018.
- [25] J. Yang, X. Shen, J. Xing, X. Tian, H. Li, B. Deng, J. Huang, and X. Hua. Quantization Networks. In *Proc. of the IEEE Conf. on Comput. Vis. and Pattern Recognit.*, 2019.
- [26] S. Zagoruyko and N. Komodakis. Wide Residual Networks. In *Proc. of the Br. Mach. Vis. Conf.*, 2016.
- [27] M. D. Zeiler and R. Fergus. Visualizing and Understanding Convolutional Networks. In *Proc. of the Eur. Conf. on Comput. Vis.*, 2014.

- [28] Y. Zhang, P. Tiño, A. Leonardis, and K. Tang. A Survey on Neural Network Interpretability. *IEEE Trans. on Emerging Topics in Computational Intell.*, 2020.
- [29] B. Zoph and Q. V. Le. Neural Architecture Search with Reinforcement Learning. In *Proc. of the International Conf. on Learn. Represent.*, nov 2017.